

Photovoltaic probe of cavity polaritons in a quantum cascade structure

Luca Sapienza,^{a)} Angela Vasanelli, Cristiano Ciuti,
Christophe Manquest, and Carlo Sirtori^{b)}

*Laboratoire Matériaux et Phénomènes Quantiques, Université Paris Diderot, Paris VII, 75205 Paris Cedex
13, France*

Raffaele Colombelli

Institut d'Electronique Fondamentale, Université Paris Sud, CNRS, 91405 Orsay, France

Ulf Gennser

Laboratoire de Photonique et Nanostructures, LPN-CNRS, Route de Nozay, 91460 Marcoussis, France

(Received 5 March 2007; accepted 26 March 2007; published online 14 May 2007)

The strong coupling between an intersubband excitation in a quantum cascade structure and a photonic mode of a planar microcavity has been detected by angle-resolved photovoltaic measurements. A typical anticrossing behavior, with a vacuum-field Rabi splitting of 16 meV at 78 K, has been measured, for an intersubband transition at 163 meV. These results show that the strong coupling regime between photons and intersubband excitations can be engineered in a quantum cascade optoelectronic device. They also demonstrate the possibility to perform angle-resolved midinfrared photodetection and to develop active devices based on intersubband cavity polaritons. © 2007 American Institute of Physics. [DOI: 10.1063/1.2739308]

Cavity polaritons are quasiparticles resulting from the strong coupling between a confined electromagnetic field and a material elementary excitation. They are the normal modes of the light-matter Hamiltonian and show a typical energy anticrossing behavior as a function of the energy detuning between the bare photon mode and the material excitation.¹ The minimum energy splitting, measured at resonance, is the so-called vacuum-field Rabi splitting. In 2003, the observation of intersubband (ISB) polaritons in reflectivity measurements was reported,² as a result of the coupling between a two-dimensional electron gas (2DEG) excitation and a photon mode in a planar microcavity based on total internal reflection.³ The same year, ISB polaritons were also observed for a bound to quasibound transition in a quantum well infrared photodetector.⁴ Because of the large oscillator strength and of the relative low energy of the ISB transitions, ISB polaritons are good candidates to explore a regime of light-matter coupling, where the Rabi frequency can be a significant fraction of the transition frequency: the so-called ultrastrong coupling regime.⁵ It is predicted that quantum electrodynamics phenomena reminiscent of the dynamic Casimir effect can be observed in this regime.^{6,7} Furthermore, recent works show a growing interest in implementing ISB polaritons in devices⁸ and the possibility of electrical control and ultrafast modulation of the ISB strong coupling regime.^{9,10}

In this letter, we report on the experimental observation of ISB cavity polaritons in angle-resolved photovoltaic measurements, performed on a quantum cascade (QC) structure embedded in a planar microcavity (Fig. 1). The QC structure is based on a GaAs/Al_{0.45}Ga_{0.55}As heterostructure, grown by molecular-beam epitaxy on an undoped GaAs (001) substrate. The planar microcavity, designed for the confinement of transverse magnetic (TM) polarized radiation, is realized by sandwiching the QC structure between a low refractive index Al_{0.95}Ga_{0.05}As layer and a top metallic mirror. In order

to measure the photogenerated voltage, circular mesas of 220 μm diameter are etched down to the bottom *n*-doped layer just below the active region. Metallic contacts are then provided on the top of the mesa and on the *n*-doped layer [Fig. 1(a)], so that electrons can be extracted directly from the structure without having to cross the Al_{0.95}Ga_{0.05}As mirror. The sample is soldered onto a copper holder and mounted on the cold finger of a cryostat, cooled at liquid nitrogen temperature. Angle-resolved measurements are performed by rotating the cold finger in order to probe cavity modes with different energies. The sample facet is polished at 70°, in order to allow a variation of the propagating angle of the incident beam over an angular range (of about 26° internal angle) useful to map the anticrossing curve.

The band diagram of the QC structure, obtained with self-consistent Schrödinger-Poisson calculations, is presented in Fig. 1(b). Photons confined within the microcavity can be absorbed promoting electrons from level 1 to level 2 of the quantum well ($E_{21}=163$ meV), with the consequent creation of ISB excitations in the 2DEG. The electronic band-structure engineering of this QC structure, analogous to that of a quantum cascade detector,¹¹ is such that electrons preferentially scatter toward one side [left side in Fig. 1(b)] of the quantum well, giving rise to a photovoltage.

In the experiment, the facet of the sample is illuminated with the radiation of a Global lamp, focused using a *f*/1.5 ZnSe planoconvex lens. The spectra are collected using a Nicolet Fourier-transform infrared spectrometer, in rapid scan mode. The inset of Fig. 2 shows three spectra collected with TM-polarized incident light at three different angles, 67.7°, 76.3°, and 81.2°. We observe a considerable variation of the shape of the spectra as a function of the angle. In Fig. 2 the solid lines are two spectra obtained with TM- and transverse electric (TE)-polarized incident light with a propagating angle of 75° with respect to the growth axis. The height of the TE curve has been adjusted following a fitting procedure that we describe later in the text. Note that the TE signal is about 20 times weaker than the TM one. Even though the polarization selection rule predicts that only TM

^{a)}Electronic mail: luca.sapienza@univ-paris-diderot.fr

^{b)}Electronic mail: carlo.sirtori@univ-paris-diderot.fr

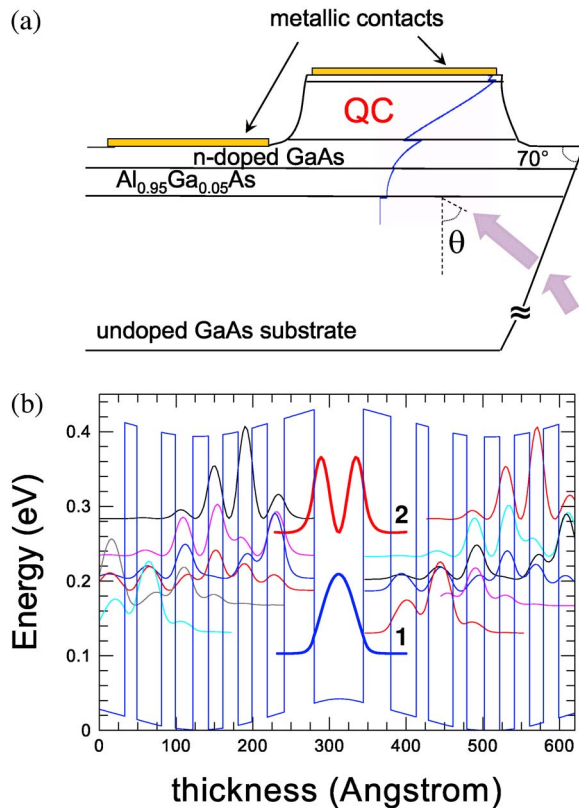


FIG. 1. (Color online) (a) Schematic view of the mesa etched sample. The layers (Si doping, thickness) from bottom to top are $\text{Al}_{0.95}\text{Ga}_{0.05}\text{As}$ (undoped, $0.52 \mu\text{m}$), GaAs ($3 \times 10^{18} \text{ cm}^{-3}$, $0.56 \mu\text{m}$), QC structure, GaAs ($1 \times 10^{17} \text{ cm}^{-3}$, 86 nm), GaAs ($3 \times 10^{18} \text{ cm}^{-3}$, 17 nm), and metallic contacts [Ni(10 nm)/Ge(60 nm)/Au(120 nm)/Ni(20 nm)/Au(200 nm)]. The arrows represent the optical path of the incident beam. The intensity of the photon mode along the growth axis is sketched (blue curve). (b) Band diagram of the QC structure. The layer sequence of one period of the structure, in nm, from left to right, starting from the largest well is **6.4/3.6/3.3/1.6/3.2/1.8/2.3/2.0/1.9/2.0/1.8/2.0/2.2/3.9**. $\text{Al}_{0.45}\text{Ga}_{0.55}\text{As}$ layers are in bold, and underlined layers are n doped with Si ($3 \times 10^{17} \text{ cm}^{-3}$). This sequence is repeated 30 times.

polarization can excite ISB transitions, we observe a spectrum from the TE polarized light, possibly because of scattering processes, occurring at the mesa sidewalls, which randomize the momentum and the polarization of the incident light.¹² This peak has the same energy position and shape in all the spectra collected at different angles and corresponds to the bare ISB transition. Moreover, the TE spectrum corresponds in shape and energy position to what can be measured very far from the anticrossing region (e.g., at 30°) and its energy position is in good agreement with the theoretical energy difference E_{21} . In fact, the TE incident light cannot be injected into the cavity mode, which is based on a surface plasmon mode [Fig. 1(a)]. The spurious TE signal that we observe must be produced by photons that have undergone a scattering event and therefore have lost their original wave vector. Hence, we are in the condition to measure the TM and the TE spectra for each angle and to subtract one another to allow a better visualization and analysis of the polaritonic contributions. This procedure has been used to obtain the spectra in Fig. 3(a), collected for different incident angles of the beam, at 78 K. A clear anticrossing between the cavity mode and the ISB excitation is visible, with a vacuum-field Rabi splitting of 16 meV.

To explain our subtracting approach, we concentrate on the TM spectrum of Fig. 2. We can distinguish the presence

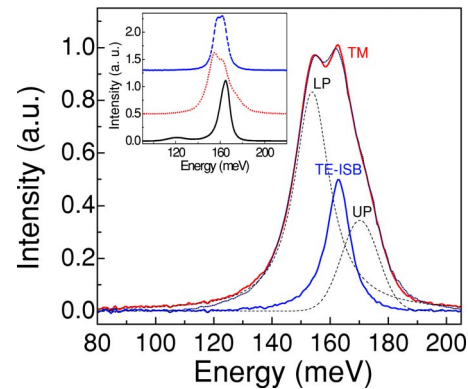


FIG. 2. (Color online) Normalized photovoltage spectra (spectral resolution of 8 cm^{-1} , at 78 K) for $\theta=75^\circ$. The solid lines labeled with TM- and TE- ISB represent the spectra collected with TM- and TE-polarized light, respectively. The two peaks in dashed lines, labeled LP and UP, are the Lorentzian and Gaussian functions, respectively, used in the fitting procedure explained in the text. The TE-ISB peak has been adjusted in height, with respect to the original spectrum, of about a factor of 5. The result of the three curve fit is shown by the dotted line. Inset: photovoltage spectra with different incident angles (67.3° solid line, 76.3° dotted line, 81.2° dashed line).

of three peaks: the lower polariton (LP, dashed line), a middle peak (TE-ISB), and the upper polariton (UP, dashed line). A three curve fitting procedure using a Lorentzian function (for the LP), a Gaussian function (for the UP), and the TE spectrum has been used to identify the height of the TE-ISB peak. The use of two different functions to obtain the best fit is due to the fact that, for the angle considered (75°), the LP is still more ISB-like and therefore Lorentzian while the UP is still more cavitylike, thus Gaussian. The fact that the cavity mode has a Gaussian shape can be explained with inhomogeneous fluctuations in the cavity dimensions, while the Lorentzian shape is typical for intersubband transitions. The fitting curve is the dotted line and shows an excellent agreement with the experimental data. Note that the Lorentzian and Gaussian shapes swap at resonance in accordance with the *light* and *matter* weight of the polaritonic wave functions [Figs. 3(b) and 3(c)]. The result of the fit indicates that the area of the spurious TE-ISB peak is 1/3 of the total area at all angles. This suggests that the bare ISB signal is proportional to the polaritonic contribution, as if it were a consequence of light scattered after polariton absorption.

This observation motivates us to underline the main differences between our experiment and the absorption experiments in which the bare ISB transition is absent.^{2,9} In absorption, the sample is unprocessed and the wave vector of both incident and collected photons are highly selected, by using lenses with long focal length. In our measurements, only the incident angle can be controlled. This implies that all the light undergoing scattering processes within the cavity can contribute to the photovoltaic signal. The reproducibility of our data has been verified on several devices and the presence of the middle peak has been observed also in different processing geometries (ridges of different sizes). The bare ISB peak is not apparent in the measurements of Ref. 4, because the authors perform a ratio between two devices with and without the cavity. This operation effectively cancels out the possible presence of the ISB peak. Further experiments and theoretical investigations are in progress to clearly identify the exact origin of this feature in our system.

In Fig. 3(b), the areas of the two polaritonic peaks, normalized to the total area, are plotted as a function of the

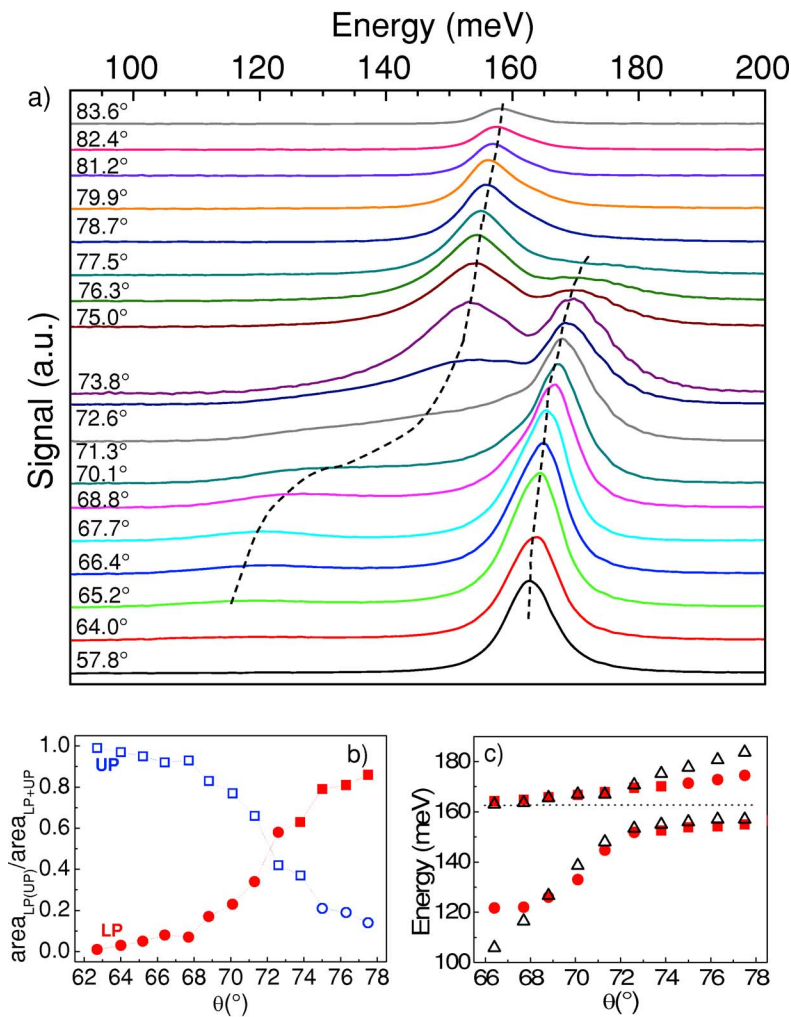


FIG. 3. (Color online) (a) Photovoltage spectra (at 78 K) obtained with TM-polarized incident radiation, after subtraction of the TE peak, presented as a function of the propagating angle within the cavity. The spectral resolution is 8 cm^{-1} and the spectra offset each other for clarity. The dashed lines are guides for the eye. (b) Areas of the UP (open symbols) and LP (full symbols) peaks, normalized to the total area, as a function of the internal angle. Squares (circles) represent values obtained using a Lorentzian (Gaussian) function in the fit. (c) Energy position of the photovoltage peaks as a function of the incident angle of the radiation (squares for Lorentzian functions, circles for Gaussian functions), compared with the results of the transfer matrix calculations (open triangles). The dashed line shows the energy of the bare ISB transition.

internal angle: the mixing of the ISB excitation and of the photon mode is evident. As expected, the upper and lower polaritons show the same area at zero detuning, when the photonic and the matter fractions are equal. In Fig. 3(c), the position of the peaks as a function of the propagating angle (full symbols) is presented, as well as the results of transfer matrix simulations (open triangles). To reproduce the experimental data, in the theoretical calculations, which take into account the dispersion of the refractive index of the Au on the surface (the Ni/Ge/Au alloy has been modeled as Au only), the electronic density has been set to $1.8 \times 10^{11} \text{ cm}^{-2}$, a lower value than the nominal one. In the transfer matrix calculations, the ISB excitation in the 2DEG has been taken into account by including in the dielectric constant of the quantum well layers, an additional term in the form of an ensemble of classical polarized Lorentz oscillators.^{2,8}

In conclusion, the results presented herein show that ISB transitions in QC structures can be used to achieve an electrical readout of states in the strong coupling regime. A signal is detected by the device only for photons impinging with a well-defined angle, allowing an angle-resolved photodetection. This represents an electrical probe of microcavity optical dynamics, with the potentiality to become an important tool for the study of cavity quantum electrodynamics in solid state systems.

The authors would like to acknowledge J. Faist, Y. Chasagneux, I. Sagnes, L. Largeau, and O. Mauguin for help and

useful discussions. They are particularly grateful to S. S. Dhillon for his help and support in the experiments. The device fabrication has been performed at the nano-center “Centrale Technologique Minerve” at the *Institut d’Electronique Fondamentale*. They gratefully acknowledge support from EU MRTN-CT-2004-51240 POISE and ANR-05-NANO-049-01 INTERPOL.

¹C. Weisbuch, M. Nishioka, A. Ishikawa, and Y. Arakawa, Phys. Rev. Lett. **69**, 3314 (1992).

²D. Dini, R. Köhler, A. Tredicucci, G. Biasiol, and L. Sorba, Phys. Rev. Lett. **90**, 116401 (2003).

³A. Liu, Phys. Rev. B **55**, 7101 (1997).

⁴E. Dupont, H. C. Liu, A. J. SpringThorpe, W. Lai, and M. Extavour, Phys. Rev. B **68**, 245320 (2003).

⁵C. Ciuti, G. Bastard, and I. Carusotto, Phys. Rev. B **72**, 115303 (2005).

⁶C. Ciuti and I. Carusotto, Phys. Rev. A **74**, 033811 (2006).

⁷S. De Liberato, C. Ciuti, and I. Carusotto, Phys. Rev. Lett. **98**, 103602 (2007).

⁸R. Colombelli, C. Ciuti, Y. Chasagneux, and C. Sirtori, Semicond. Sci. Technol. **20**, 985 (2005).

⁹A. A. Anappara, A. Tredicucci, G. Biasiol, and L. Sorba, Appl. Phys. Lett. **87**, 051105 (2005).

¹⁰A. A. Anappara, A. Tredicucci, F. Beltram, G. Biasiol, and L. Sorba, Appl. Phys. Lett. **89**, 171109 (2006).

¹¹L. Gendron, M. Carras, A. Huynh, V. Ortiz, C. Koeniguer, and V. Berger, Appl. Phys. Lett. **85**, 2824 (2004).

¹²H. C. Liu, M. Buchanan, and Z. R. Wasilewski, Appl. Phys. Lett. **72**, 1682 (1998).